*27th European Conference on Optical Communication (ECOC 2001), Sept. 30-Oct. 4, 2001, Amsterdam, the Netherlands, paper Th.F.2.1 (**Invitede Talk**).*

Ultrahigh-speed all-optical data regeneration and wavelength conversion for OTDM systems

Y. Ueno, S. Nakamura, J. Sasaki, T. Shimoda, A. Furukawa, T. Tamanuki, T. Sasaki, and K. Tajima

Photonic and Wireless Devices Research Laboratories, NEC Corporation
34 Miyukigaoka, Tsukuba, Ibaraki 305-8501, Japan (y-ueno@cb.jp.nec.com)

Abstract: The latest results in ultrafast data regeneration and wavelength conversion with SMZ-type all-optical semiconductor switches are reviewed. In these operations, the SMZ-type switch is driven by random data pulses. The fastest bit rate reported to date for such input-data-driven all-optical operation has reached 168 Gb/s. With these all-optical devices, we may be able to build 160-Gb/s OTDM nodes for packet communications systems in the near future.

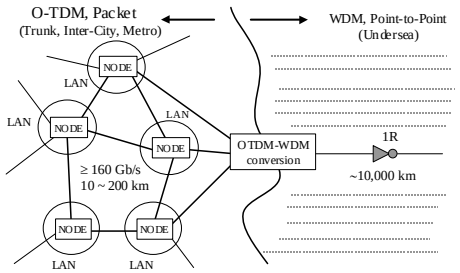

Figure 1: OTDM-based mesh networks

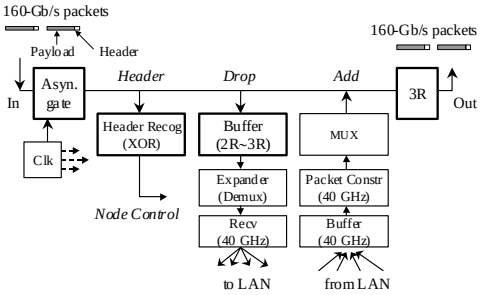

Figure 2: Example of OTDM-based node system

1. Introduction : OTDM networks beyond 40 Gb/s/ch

Ultrafast optical-time-division-multiplexing (OTDM) technology is very attractive in that it provides bandwidths that are not limited by opto-electronic devices, leads to more flexible TDM packet networks, and reduces the number of cross connections required in multi-Tb/s WDM systems (Fig. 1). A number of essential ultrafast all-optical functions, including demultiplexing [1-5], wavelength conversion [6-13], 3R regeneration [13-18], and OTDM-WDM conversion [19], have been demonstrated and studied. All of the all-optical devices in the reports cited above are based on interferometric semiconductor switches of the Symmetric-Mach-Zehnder (SMZ) type [1, 2, 7]. These switches form rectangular-like switch windows, in principle, with ultrafast response times (rise and fall times). The response time is not limited by the slow semiconductor carrier relaxation times, because optical interference inside each device masks the slow-relaxation-induced optical components. Some of the works cited above were done at or below 40 Gb/s but the bit rate in research experiments is shifting from 40 Gb/s to the 80-160 Gb/s range [4, 5, 10-13, 15, 18], with the aim of providing devices for use in the OTDM-based network systems.

Figure 2 shows an example of an OTDM-based node system for packet communications that we may be able to build with the above-mentioned SMZ-type devices. An SMZ all-optical switch inside a packet-expander unit [20] will demultiplex and expand 160-Gb/s OTDM packets to packets at ETDM bit rates. A switch of the same type is also applicable to 3R regeneration and makes the system more tolerant to GVD, PMD, XPM, and ASE noise accumulation. The 3R regenerator will be a key component of the optical buffer (regenerative buffer), too. The SMZ switch also works as an asynchronous gate [21] because of its jitter-tolerence. Furthermore, SMZ-type wavelength convertors will cross-connect the OTDM signals between WDM channels.

In this report, we review the latest results in 3R regeneration, wavelength conversion with SMZ-type switches, and some of the related topics in this field.

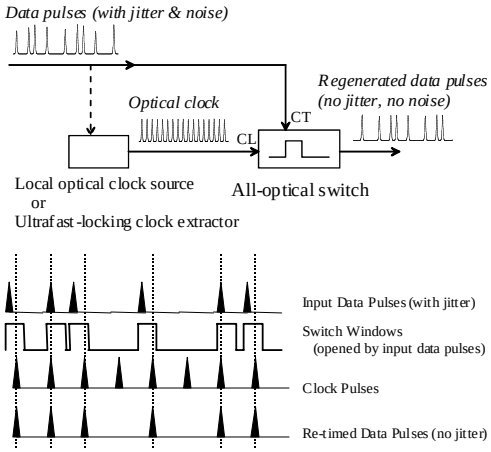

Figure 3: All-optical 3R scheme (top) and re-timing feature required for the switch (bottom)

2. The principle of 3R regeneration and the mechanism of the SMZ all-optical switch

Figure 3 shows how an ideal 3R regenerator (re-amplification, re-shaping, and re-timing) functions. The all-optical switch receives data and clock pulses so that the data pulses all-optically encode the stream of clock pulses. Suppose the clock pulses have no timing jitter, while the input data pulses have some jitter. As each data pulse forms a rectangular-like switch window with respect to the clock pulses, the timing jitter in the input data pulses is removed

(i.e., re-timed). Furthermore, when the transmissivity of the switch window does not depend on a specific range of intensity fluctuation of the input data pulses, the intensity fluctuation is also removed (re-shaped). These are the two features that are required for all-optical switches used in 3R regeneration.

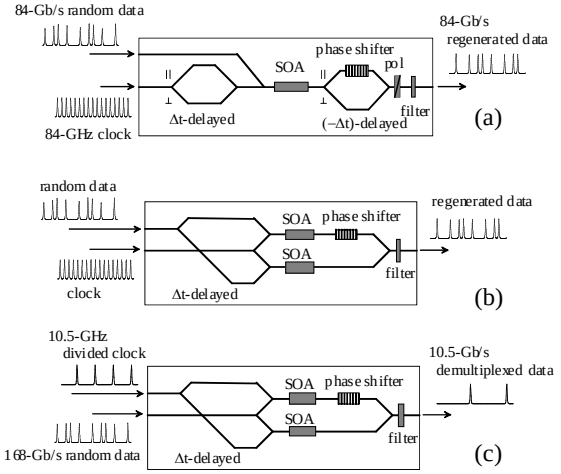

Figure 4: (a) PD-SMZ switch for 3R, (b) SMZ switch for 3R, and (c) SMZ switch for demultiplexing.

Figure 4(a) shows a schematic view of one of the SMZ-type switches, a polarization-discriminating Symmetric-Mach-Zehnder (PD-SMZ) all-optical switch [2], and its input scheme for 3R regeneration [15, 18]. The switch consists of a semiconductor optical amplifier (SOA) and a pair of polarization-dependent delay lines (PDD). Each time a data pulse is amplified in the SOA, the refractive index of the SOA's active layer increases and then relaxes due to the band-filling effect induced by a carrier-density change. Here, the rise time of the refractive-index change is as fast as the width of the data pulse while its relaxation is relatively slow. Each successive clock pulse is split into two orthogonally-polarized pulses in the first PDD. After one of the two-split pulses is given a delay time Δt with respect to the other pulse, the two-split pulses are recombined at the PDD output. The two-split Δt-spaced orthogonally-polarized pulses are then amplified by the SOA and enter the second PDD. In the second PDD, the delay time between the two-split pulses is compensated. As a result, the two-split pulses are recombined at the second PDD's output and then interfere with each at the 45° polarizer output. Thus, the pair of PDDs work as a MZI (with respect to clock pulses). The optical phase of this MZI is initially biased so that the two-split pulses either destructively or constructively interfere with each other. When a data pulse co-propagates between the two-split Δt-spaced pulses, the one pulse experiences the nonlinear refractive-index change while the other pulse does not and consequently the initial interference condition changes. The data pulses thus all-optically encode the co-propagating clock pulses via the PD-SMZ switch. Due to the interference between the two-split pulses, the switch effectively masks the slow relaxation of the refractive-index and forms a rectangular-like switch window. The switch window's width is passively determined by the pulse-propagation delay time (Δt) between the two delay lines of the PDD's. All of the PD-SMZ switches reported previously were not integrated (on a chip) but built by experimentally combining an SOA (or a semiconductor waveguide) with a pair of matched birefringent crystals (or panda fibers), polarizers, etc.

Figures 4(b) and 4(c) show the original SMZ switch [1], for comparison. With the input scheme in Fig. 4(b), the switch works for the 3R regeneration [14]. With the input scheme in Fig. 4(c), it works for demultiplexing [4]. The switch window's width in the SMZ switch is pre-determined by the delay time (Δt) between the two asymmetric input arms in Figs. 4(b) and 4(c).

The nonlinear refractive-index changes inside SMZ-type switches for the 3R operation, wavelength conversion, and asynchronous gating must be repeated at the ultrafast OTDM data rate and this is in contrast to the situation for demultiplexing. Furthermore, SMZ switches for the 3R operation, etc. are controlled by random data pulses while those for demultiplexing are controlled by regular (continuous) clock pulses. Data-pattern-induced effects are thus a potential problem for the SMZ switches for 3R, etc. The pattern-induced effects are suppressed by accelerating the carrier relaxation with increasing the input clock-pulse power [14].

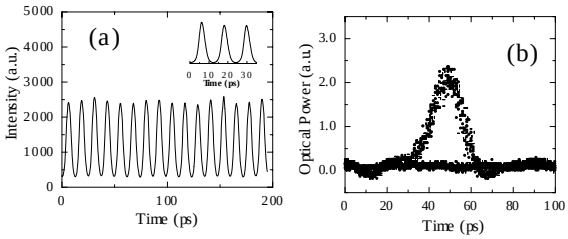

Figure 5: Waveforms of 84-Gb/s regenerated data (a) and eye diagram after demultiplexing to 10.5-Gb/s (b)

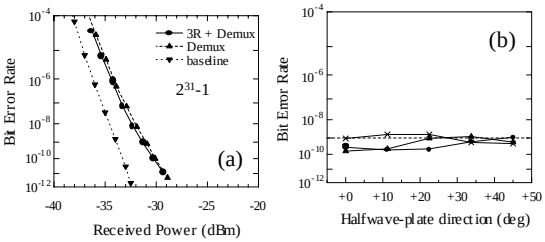

Figure 6: Measured bit-error rates

3. Experimental results in 3R regeneration

Figure 5(a) shows average waveforms, as observed with a high-speed streak camera, of 84-Gb/s pseudorandom data pulses regenerated by the PD-SMZ switch in Fig. 4(a) [13, 18]. The extinction ratio for the regenerated pulses was 17 dB, as indicated in the inset. Figure 5(b) shows a typical eye diagram of regenerated data after demultiplexing from 84 to 10.5 Gb/s with the hybrid-integrated SMZ switch in Ref. 4. The input powers of the 84-Gb/s 1560-nm data and the 84-GHz 1545-nm clock pulses coupled to the SOA were –4 dBm and +2 dBm, respectively. The switch-window width was set to half of the repetition time (Δt= 6.2 ps). The optical phase of the MZI inside the switch was biased so that an input '1' pulse would be inverted to a '0' pulse at the output and vice versa (inversion operation).

The solid curve in Fig. 6(a) shows measured bit-error rates of the renegerated and demultiplexed 10.5-Gb/s data pulses of Fig. 5(b). The length of the pseudorandom pattern was set to 2^{31}-1. For comparison, the dashed curve shows

those of demultiplexed 10.5-Gb/s data pulses without 3R regeneration, while the dotted curve indicates the 10.5-Gb/s baseline of our detection system. Although the all-optical demultiplexer exhibited a slight power penalty, the penalty of the 3R regeneration in itself (the difference between the solid and dashed curves) was negligibly small.

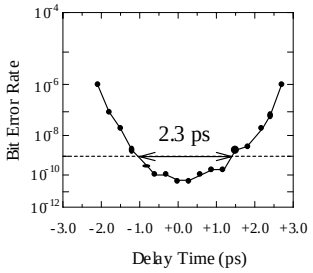

Figure 7: Tolerence to input-timing jitter

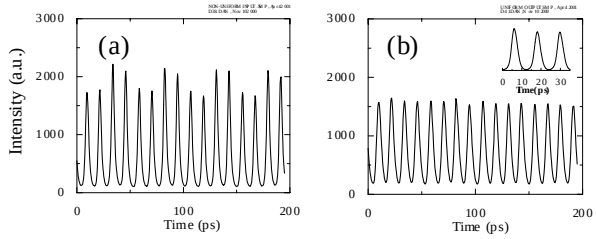

Figure 8: Re-shaping capability of the PD-SMZ switch

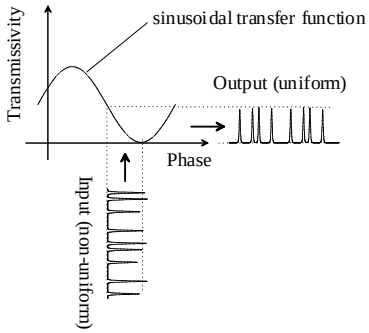

Figure 9: Mechanism of the re-shaping shown in Fig. 8

It should be noted here that the PD-SMZ switch in Fig. 4(a) is, in principle, polarization-insensitive to the input data pulses when a polarization-insensitive SOA is used. Our experiment proved this: the measured bit-error rate depended very little on the polarization state of the input data pulses [Fig. 6(b)]. Here, half-wave and quarter-wave plates were used to rotate the polarization state of the 84-Gb/s input data pulses around the Poincare sphere.

Figure 7 indicates the re-timing capability of the PD-SMZ switch, where the bit-error rate was measured as a function of the relative delay time between the data and clock pulses. The bit error rates remained below 10^{-9} even when the data pulses were delayed by 2.3 ps. This amount of jitter tolerence is reasonable with the switch window width (Δt= 6 ps) and the data pulse width (2.0 ps), because the rise and fall times of the 'rectangular-like' switch window are close to the data-pulse width.

Figure 8 indicates the re-shaping capability of the PD-SMZ switch. Here, 84-Gb/s pseudorandom input data pulses having non-uniform peak intensities were intentionally generated [Fig. 8(a)]. As indicated in Fig. 8(b), the non-uniformity was sucessfully removed from the regenerated pulses.

Although the intensity fluctuation in the input 1's is absent in Fig. 8(b), we found that our PD-SMZ switch only partially re-shapes the 84-Gb/s data pulses at present: the intensity fluctuation in the input 0's is not removed but is transferred to the output 1's (in the inversion operation). This is because the nonlinear phase shift of our 3R regeneration at 84 Gb/s was compressed to below π, in contrast to the result at 20 Gb/s in Ref. 14. In fact, the nonlinear phase shift in the 84-Gb/s 3R operation was measured as 0.4-0.6π. We interpreted these results in the following way: (a) even when the nonlinear phase shift is less than π, either 0's or 1's are re-shaped due to the MZI's sinusoidal transfer function, as is schematically shown in Fig. 9. (b) When the nonlinear phase shift reaches π, both 0's and 1's are re-shaped. According to these results, we suggest that the re-shaping properties of any SMZ switch should be investigated separately for 0's and 1's. Measuring the nonlinear phase shift helps in physically understanding how each pulse is re-shaped.

The data and clock pulses in all of the above 3R experiments were generated by using a pair of synchronized pulse sources. In the next section, we address potential techniques for generating the optical clock in a real 3R system.

4. Clock pulse generation for 3R systems

To date, synchronization and clock-extraction techniques of many types have been proposed and demonstrated for use with ultrafast optical signals. Here, we introduce a few of them, divided into two alternative strategies.

When the packets are relatively short, we may be able to use a local clock source and operate all of the node functions asynchronously (Fig. 2). At the node input, an SMZ switch having a specific jitter tolerence works as an asynchronous gate. Via this asynchronous gate, the local clock pulses are all-optically encoded by the asynchronous input data packets. This works when the data frequency is close enough to the clock frequency and the packet is short enough [21]. Thus, the asynchronous gate converts the input data packets from asynchronous to synchronous form and then passes them to other units or to neighbour systems, without having to extract clocks from the packets.

When the packets are relatively long, we may be able to use an all-optical clock extractor to extract optical clock pulses very quickly from ultrafast packets. One promising technique for ultrafast clock extraction is the application of self-pulsation lasers: locking times within some tens of bits have recently been reported [22]. Other possible clock extractors are those with SOA-based ring structures, where an SOA works as a nonlinear element [23, 24]. The locking time can be reduced dramatically by integrating each ring structure into a small chip and thus reducing the pulse circulation time. An SMZ-type switch is used in one of the above reports [24], where the extracted clock-pulse width is stabilized by the pre-determined delay time Δt of the switch.

5. Wavelength conversion

With SMZ-type switches, as implied above, the wavelength of the data pulses is converted to that of the clock pulses each time they are regenerated. Thus, one can convert the wavelength at the 3R unit and the asynchronous gate unit in designing the node in Fig. 2.

Separately, a very compact wavelength convertor, the delayed-interference signal-wavelength convertor (DISC [7]) in Fig. 10, has been exhibiting ultrafast performance. The mechanism of this wavelength convertor is similar to that of the original SMZ switch. The optical interference masks the carrier-induced relaxation time of the SOA. The width of the all-optically-formed switch window is determined by a delay time Δt between the two arms of the asymmetric MZI. With a pseudorandom input, it slices the co-propagating continuous-wave (CW) light and consequently generates wavelength-converted pseudorandom data pulses.

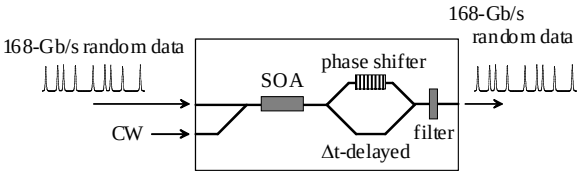

Figure 10: The DISC wavelength converter

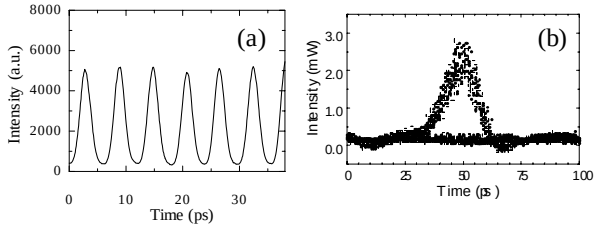

Figure 11: Average waveform of the 168-Gb/s wavelength-converted data (a) and the eye diagram after demultiplexed to 10.5-Gb/s (b)

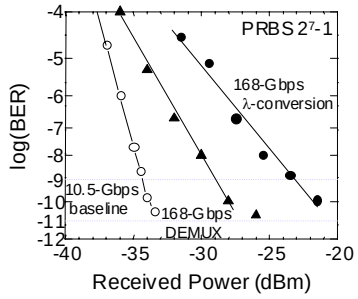

Figure 12: Measured bit-error rates in the 168-Gb/s wavelength-conversion process

Figure 11(a) shows an averaged waveform of the 168-Gb/s pseudorandom data pulses after wavelength conversion from 1564 to 1547 nm [13]. The input powers of the 168-Gb/s data pulses and the CW light were +7 dBm and +13 dBm, respectively. The output pulses' extinction ratio was 13 dB. The input and output data-pulse widths were measured with an autocorrelator as 1.8 and 2.0 ps, respectively (the output pulse width matched well with Δt). Nevertheless, the nonlinear phase shift involved in this wavelength conversion was less than that seen in the PD-SMZ switch during 84-Gb/s 3R operation.

Figure 11(b) shows a clear eye opening in the wavelength-converted and demultiplexed 10.5-Gb/s data pulses. Under these operating conditions, error-free wavelength conversion at 168 Gb/s was successfully achieved (Fig. 12). To the authors' knowledge, this was the first error-free operation of any all-optical switch driven by random data pulses at 160 Gb/s.

6. Technical issues

The decrease in the nonlinear phase shift inside the SOA with the switch-repetition rate is one of the issues in both 3R regeneration and wavelength conversion, although it has not been discussed enough in the literature. We believe that we can improve the nonlinear phase shift at 160 Gb/s and at even higher rates by re-designing the SOA for all-optical purposes. The pulse-width tunability, wavelength tunability, and timing jitter of current short pulse sources are other technical issues for research into these ultrafast devices. Advances in these technical areas will be a further drive for the research activity in this field.

7. Conclusion

We have reported on the latest results in 3R and wavelength conversion. The successful 168-Gb/s data-pulse-driven random operation of an SMZ-type all-optical switch (a wavelength convertor) has suggested that we are approaching the possibility of building 160-Gb/s node systems that contain 3R regenerators, asynchronous gates, and wavelength convertors.

This work was performed partially under the management of the Femtosecond Technology Research Association (FESTA) supported by the New Energy and Industrial Technology Development Organization (NEDO).

References

/1/ K. Tajima, Jpn. J. Appl. Phys. **32** (1993) L1746.
/2/ K. Tajima et al., Appl. Phys. Lett. **67** (1995) 3709.
/3/ S. Nakamura et al., IEEE Photonics Technol. Lett. **10** (1998) 1575.
/4/ S. Nakamura et al., IEEE Photonics Technol. Lett. **12** (2000) 425.
/5/ R. Ludwig et al., Electron. Lett. **36** (2000) 1405.
/6/ B. Mikkelsen et al., Electron. Lett. **33** (1997) 2137.
/7/ Y. Ueno et al., IEEE Photonics Technol. Lett. **10** (1998) 346.
/8/ Y. Ueno et al., Opt. Lett. **23** (1998) 1846.
/9/ Y. Ueno et al., Jpn. J. Appl. Phys. **38** (1999) L1243.
/10/ Y. Ueno et al., Jpn. J. Appl. Phys. **39** (2000) L806.
/11/ J. Leuthold et al., Electron. Lett. **36** (2000) 1129.
/12/ Y. Ueno et al., ECOC 2000, Munich, pp. 13-15.
/13/ S. Nakamura et al., Optical Amplifiers and their Applications, July 9-12, 2000, Quebec, PD4-1.
/14/ L. Billes et al., ECOC '97, Edinburgh, Vol. 2, 269.
/15/ A.E. Kelly et al., Electron. Lett. **35** (1999) 1477.
/16/ D. Wolfson et al., IEEE Photonics Technol. Lett. **12** (2000) 332.
/17/ St. Fisher et al., IEEE Photonics Technol. Lett. **12** (2000) 335.
/18/ Y. Ueno et al., IEEE Photonics Technol. Lett. **13** (2001) 469.
/19/ St. Fisher et al., IEEE Photonics Technol. Lett. **11** (1999) 1262.
/20/ A. Hasegawa and H. Toda, IEICE Trans. Commun. **E81-B** (1998) 1681.
/21/ D. Cotter and A. Ellis, J. Lightwave Technol. **16** (1998) 2068.
/22/ B. Sartorius, OFC 2001, Anaheim, MB7.
/23/ K. Vlachos et al., OFC 2000, Baltimore, ThP2.
/24/ Y. Ueno et al., Jpn. J. Appl. Phys. **39** (2000) L803.